Organic & Biomolecular Chemistry

PAPER

View Article Online
View Journal | View Issue

Cite this: *Org. Biomol. Chem.*, 2015, **13**, 1732

Aryl-bis-(scorpiand)-aza receptors differentiate between nucleotide monophosphates by a combination of aromatic, hydrogen bond and electrostatic interactions†

Jorge González-García,[a] Sanja Tomić,[b] Alberto Lopera,[a] Lluís Guijarro,[a] Ivo Piantanida*[c] and Enrique García-España*[a]

Received 30th September 2014,
Accepted 26th November 2014

DOI: 10.1039/c4ob02084g

www.rsc.org/obc

Bis-polyaza pyridinophane scorpiands bind nucleotides in aqueous medium with 10–100 micromolar affinity, predominantly by electrostatic interactions between nucleotide phosphates and protonated aliphatic amines and assisted by aromatic stacking interactions. The pyridine-scorpiand receptor showed rare selectivity toward CMP with respect to other nucleotides, whereby two orders of magnitude affinity difference between CMP and UMP was the most appealing. The phenanthroline-scorpiand receptor revealed at pH 5 strong selectivity toward AMP with respect to other NMPs, based on the protonation of adenine heterocyclic N1. The results stress that the efficient recognition of small biomolecules within scorpiand-like receptors relies mostly on the electrostatic and H-bonding interactions despite the competitive interactions in the bulk solvent, thus supporting further optimisation of this versatile artificial moiety.

Introduction

Nucleotides are among the most targeted anionic substrates due to the key roles that they play in biology such as nucleic acid synthesis, transport across membranes, and energy and electron-transfer events. Other relevant functions of nucleotides are related to cell-signalling processes.[1] In this respect, the extracellular release of nucleotides serves as a signal during inflammation through the activation of nucleotide receptors P1 and P2.[2] Transmembrane protein channels have been implicated in the release of adenosine nucleotides from the intra- to the extracellular space in apoptotic cells.[3] In addition, several studies have proved the release of uridine nucleotides during cystic fibrosis.[4] Therefore, the development of new abiotic receptors that are able to selectively bind nucleotides in aqueous solution is a relevant goal in chemical and biomedical research.[5]

The interaction among naturally occurring nucleobases and abiotic receptors occurs mainly through columbic interactions, hydrogen bonding and π–π stacking. Very good examples of the involvement of different forces in nucleotide binding are provided by the crystal structures of adducts formed between protonated terpyridinophane or phenanthroline macrocycles with 5′-thymidine triphosphate (5′-TTP).[6]

Since the dominant driving force in nucleotide binding is charge–charge interaction, a great deal of the studies reported so far describe the selection of the more charged nucleotides with respect to the less charged ones.[7–10] Reversed selectivity of ADP over ATP in water was recently reported to occur through the synergistic action of the different binding groups included in a tris(2-aminoethyl)amine receptor containing a pyrimidine group.[11]

A case of selectivity for AMP over ADP and ATP as a result of strong electrostatic contacts supported by π–π interactions was recently reported in a guanidinium-polypeptide-based polytopic receptor.[12]

However, achieving base-pair discrimination is a challenging target in biomedical and supramolecular chemistry. Very often base-pair discrimination relies on different hydrogen bonding patterns between the partners which limit its effectivity in water due to competitive hydrogen bonding with the solvent.[13] To overcome this difficulty, several years ago

[a]*ICMOL, Departamentos de Química Inorgánica y Orgánica, Facultad de Química, Universidad de Valencia, C/Catedrático José Beltrán 2, 46980 Paterna, Valencia, Spain. E-mail: enrique.garcia-es@ uv.es*
[b]*Laboratory for Chemical and Biological Crystallography, Division of Physical Chemistry, Ruđer Bošković Institute, HR 10002 Zagreb, Croatia*
[c]*Laboratory for Study of Interactions of Biomacromolecules, Division of Organic Chemistry and Biochemistry, Ruđer Bošković Institute, Zagreb, Croatia. E-mail: pianta@irb.hr*

†Electronic supplementary information (ESI) available: Electronic fluorimetric data and potentiometric titrations, detailed experimental conditions, NMR analyses and molecular modelling. See DOI: 10.1039/c4ob02084g

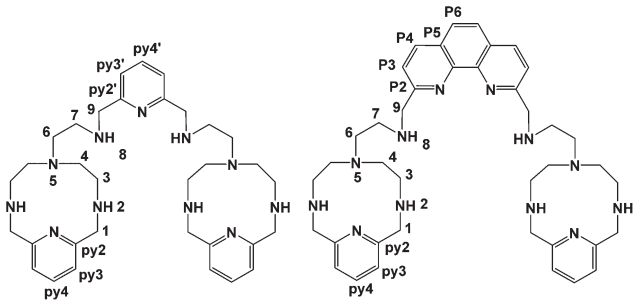

Scheme 1 Studied **PYPOD** (left) and **PHENPOD** (right).

sapphyrin and calixpyrrole derivatives appended with nucleobases were designed so that the interaction with the complementary nucleotide was enhanced by hydrogen bonding.[14] Favourable discrimination of AMP over the other nucleotide monophosphates (NMPs) by hydrogen bonding was reported using a polytopic receptor with a bis(oxazolin-2-yl)pyridine scaffold.[15]

Several bis-intercaland-type macrocycles constituted another example of nucleobase discrimination.[16] In this work, particularly interesting is the selectivity toward certain nucleobases ascribed to the interaction of the bases with the polyamine-linkers connecting the intercalating subunits.[17]

On the other hand, Kimura and co-workers reported for the first time, the ability of the Zn^{2+} complex of cyclen to interact selectively with thymine and uracil through metal ion coordinative bonding to the deprotonated imide group and hydrogen-bonding formation between the amine groups and the pyrimidine carbonyl groups.[18] These findings led to development of cyclen derivatives, either with aromatic groups appended in their structure or with more than one cyclen unit.[19]

Recently, some of us have designed a series of scorpiand-like receptors with different appended motifs in the tail able to discriminate certain nucleobases due to a predominant hydrogen bonding or π–π stacking interaction.[20]

A further development of the scorpiand-like receptors just mentioned are the double bis-scorpiand receptors **PYPOD** or **PHENPOD**, built by connecting two macrocyclic units containing pyridine moieties with pyridine or phenanthroline linkers, respectively (Scheme 1).[21] These compounds, particularly **PYPOD** which have shown selectivity of RNA over DNA,[22] are examined in this work for their capability to achieve base-pair discrimination in the recognition of NMPs. The selectivity is analysed in terms of how the functionalities present in the receptors complement AMP, GMP, UMP or CMP.

Results and discussion

Acid–base properties of the nucleotide monophosphates

Before performing any speciation study, it was necessary to calculate the protonation constants of the different NMPs under the same experimental conditions used in the work (Table S1,† NaCl 0.15 M at 298.0 K).

From potentiometric analysis, we obtained the protonation constants of the phosphate groups (between 6.1 and 6.3, depending on the nucleotide, see Table S1†) and the stepwise protonation constants of the deprotonated imide nitrogen in the heterocyclic base of GMP and UMP.[23] Moreover, the protonation constants of nitrogen N1 in the aromatic ring of AMP and CMP were also determined.[24] To confirm these values and get structural information about the protonation sites of the nucleotides, pH dependent ^{1}H and ^{31}P NMR spectra (ESI Chart 1 for labelling and Fig. S1–S5†) were registered in deuterated water. The protonation constants were obtained by treatment of the ^{1}H and ^{31}P NMR chemical shifts at different pD values with the HyperNMR software (Table S1†).[25] The values obtained were in reasonable agreement with those calculated by pH-metric analysis.

Interaction of PHENPOD and PYPOD with nucleotide monophosphates

Potentiometric and fluorimetric studies. The interaction of the positively charged receptors with the negatively charged NMPs has been first investigated by potentiometric studies. The analysis of the pH-metric titrations with the HYPERQUAD set of programs gave the model and values of the cumulative constants reported in Table S2.†[26] Receptor–nucleotide adducts of H_xLA stoichiometries, where x varied from 1 to 7 for **PYPOD** and from 1 to 8 for **PHENPOD**, were found for all the systems. The higher protonated degrees observed in the **PHENPOD**–NMP systems can be attributed to the higher protonation degree achieved by this receptor; while free **PHENPOD** reaches a protonation degree of 7, **PYPOD** only reaches a protonation degree of 6. The distribution diagrams in Fig. S6 and S7† show the existence of adducts over a wide pH range.

Since both the substrates and the receptors participate in overlapped proton transfer processes, translating the cumulative stability constants into representative stepwise constants is not always straightforward. To do this, the basicity constants of both the substrate and the receptor have to be taken into account and it should be assumed that the interaction will not greatly affect the pH range of existence of the protonated species of nucleotides and receptors. In this way, the stepwise constants (Table S3†) have been calculated for **PHENPOD**–NMP and **PYPOD**–NMP systems. Nevertheless, the most unambiguous way to compare the relative stabilities of the different systems and to establish selectivity ratios at different pH values is to use effective constants (K_{eff}). The effective constants are calculated at each pH value as the quotient between the overall amount of complexed species and the overall amounts of free receptors and substrates, independent of the protonation degree (Fig. 1).[27]

The effective constants for all the **PYPOD**–NMP systems show bell-shaped profiles with maximum values of the effective constants in the 6–8 pH range. At higher pH values the positive charge in the receptor would not be high enough

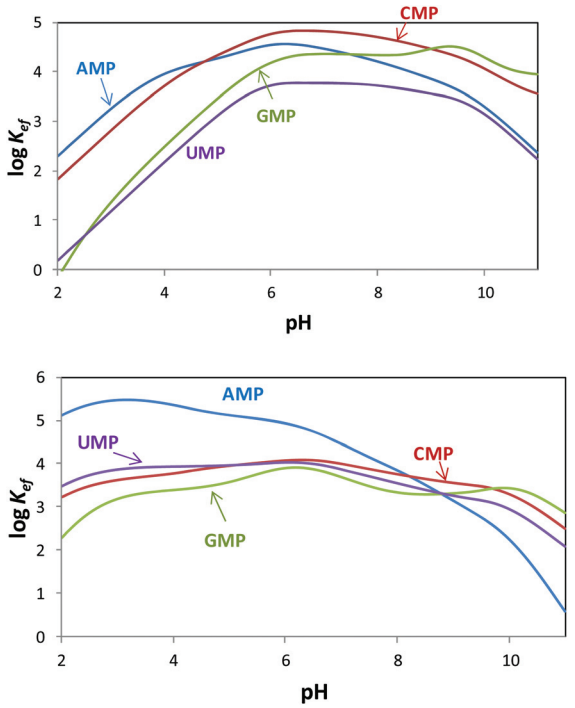

Fig. 1 Plot of the pH dependence of effective constants (log K_{eff}/M^{-1}) for the systems **PYPOD** (up) or **PHENPOD** (down) with AMP, GMP, CMP and UMP.

to achieve a strong interaction. On the other hand, at pH values below 6 the nucleotide starts to protonate by reducing its negative charge. For the **PHENPOD**–NMP systems, in particular for AMP, the log K_{eff}-pH profile is different. Although the profile is still bell-shaped the stability observed at acidic pH values is significantly higher, which can likely be attributed to π–π stacking and to the hydrophobicity afforded by the larger condensed aromatic phenanthroline ring. While in the case of **PYPOD** the situation is not so apparent, **PHENPOD** clearly recognises AMP over the other three mononucleotides below pH = 8.

In this regard, while the fluorescence emission of **PYPOD** is too low to perform fluorimetric titrations at any pH value, the intrinsic fluorescence emission of **PHENPOD** allowed us to carry out titrations with the nucleotides at acidic pH values (Fig. 2). The addition of the nucleotides to a solution of **PHENPOD** at pH = 5 leads to a decrease in fluorescence which was particularly noticeable for AMP (Fig. 2). Such quenching processes can be attributed to hydrogen bonding and charge interactions between the anionic phosphate moiety and the polyammonium chain of the protonated receptor, which could lead to an intra-complex proton transfer from an ammonium group to a phosphate group making an amine lone pair available for the quenching process.[6b] The effective constants calculated by processing the fluorimetric data with the HypSpec program that are collected in Table 1 are in reasonable agreement with the values derived from the pH-metric titrations and confirm the selective recognition of AMP by **PHENPOD**.

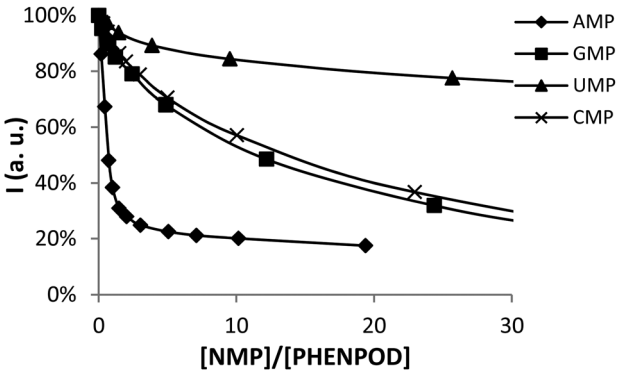

Fig. 2 Plot of the fluorescence intensity normalized *vs.* the molar ratio [NMP]/[**PHENPOD**].

Table 1 Calculated values of the logarithms of the effective stability constants for the interaction of nucleotide monophosphates with **PYPOD** and **PHENPOD** determined at 298.0 ± 0.1 K in 0.15 M NaCl at pH = 5.0 and 7.0

	pH = 5.0		7.0	
	PYPOD	PHENPOD	PYPOD	PHENPOD
AMP	4.28	5.11 (5.63 (6))[a]	4.45	4.44
GMP	3.51	3.60 (3.52 (2))[a]	4.35	3.67
CMP	4.37	3.96 (3.46 (2))[a]	4.82	3.99
UMP	3.16	3.95 (3.59 (6))[a]	3.76	3.84

[a] Calculated from fluorimetric titrations. Values in the brackets inside are standard deviations of the last significant figure.

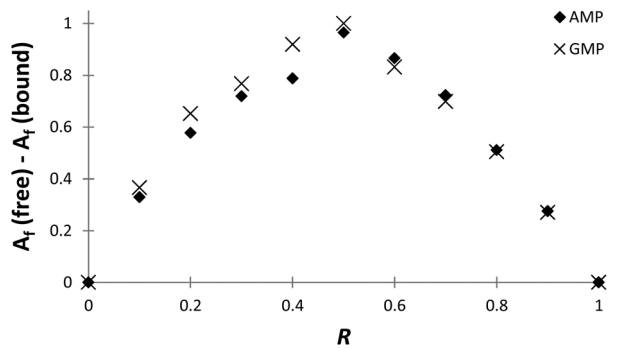

Fig. 3 Job plot for complex formation between **PHENPOD** and AMP (♦) or GMP (×). Spectra were recorded at 369 nm in a pH 5.0 solution (0.05 M cacodylate buffer) at a total concentration of [**PHENPOD**] + [NMP] = 5×10^{-5} M.

The stoichiometries of the **PHENPOD**–NMP systems were further confirmed by fluorescence emission techniques using Job plots (continuous variation experiments) at pH 5.[28] For this purpose, $\Delta A_f = A_f$ (free) − A_f (bound) was plotted against the ratio of concentrations R = [L]/([L] + [NMP]), in which A_f is the area of the fluorescence emission peaks of **PHENPOD**, free or bound to the nucleotide, at a constant total ([L] + [NMP]) concentration[29] (Fig. 3 and Fig. S8†). In all cases, a maximum

is observed at 0.5 supporting a 1 : 1 stoichiometry. Similar conclusions were derived from Job plots obtained with ^{1}H NMR data (Fig. S11 and S12†).

Regarding the pyrimidine nucleotides, the plot of the effective constants reveals an unexpectedly high selectivity of **PYPOD** for CMP over UMP throughout the complete pH range, K_{eff} for CMP being an order of magnitude higher than for UMP (see Fig. 1). This selectivity could originate from different hydrogen bonding patterns of CMP and UMP. Furthermore, since the **PYPOD**–CMP complex is, under physiological conditions (pH = 6–8), about 3–5 times more stable than the complexes with the purine-nucleotides (AMP and GMP), contribution of aromatic stacking between **PYPOD** and the nucleobase is not a dominant binding interaction controlling the overall stability of the **PYPOD**/NMP complex formed.

The selectivity for CMP completely disappears when the central pyridine unit (**PYPOD**) is substituted by phenanthroline (**PHENPOD**). In the binding mode of **PHENPOD** with purines (AMP, GMP), the phenanthroline moiety plays a crucial role interacting with the base by aromatic stacking as confirmed by the NMR experiments (see below). Therefore, the adducts formed in the **PHENPOD** : purine systems adopt a forced conformation, reducing the impact of electrostatic interactions in comparison with pyridine nucleotides. The high selectivity of **PHENPOD** for AMP under acidic conditions (pH < 5.5) most likely involves the protonation of adenine at the N1 position. Indeed, it has been observed that adenine heterocycles self-stack more efficiently when 50% of the adenine moieties are protonated at N1.[30] The same analogy could be used to explain the preferred stacking between the N1-protonated adenine with the neutral phenanthroline ring in comparison with the non-protonated guanine. Moreover, the data of purine/pyrimidine self-stacking for nucleosides show the trend A > G > T > C, reflecting the decreasing aromaticity and hydrophobic character of their nucleobase residues supporting the stacking preference of adenine for **PHENPOD**.[30]

NMR experiments. For a better insight into the structure of the complexes formed and their pH dependences, ^{1}H and ^{31}P NMR spectra were collected in D_2O (for the atom labelling see Scheme 1 and Chart 1 in ESI†). The results showed major ^{1}H/^{31}P NMR shift differences between the signals of the complexes and of the free nucleotides and ligands in the 6.7–7.2 pH range, again confirming the complex formation. As an example, Fig. 4 and Fig. S10† show the variation in the ^{31}P NMR signal at different pD values for the free nucleotides and for the complexes with the different NMPs. It should be noted that the formation of a ligand/NMP complex changes the pK values of both the ligand and the nucleotide at positions involved in the interaction.

Furthermore, the ^{1}H NMR shifts of the aromatic signals of solutions of the nucleotides and receptors in 1 : 1 molar ratio (Fig. 5a and b) revealed more pronounced shifts for the **PHENPOD**–NMP systems than for the **PYPOD**–NMP systems, suggesting a stronger aromatic stacking between the nucleobases and the phenanthroline. The anomeric proton signal

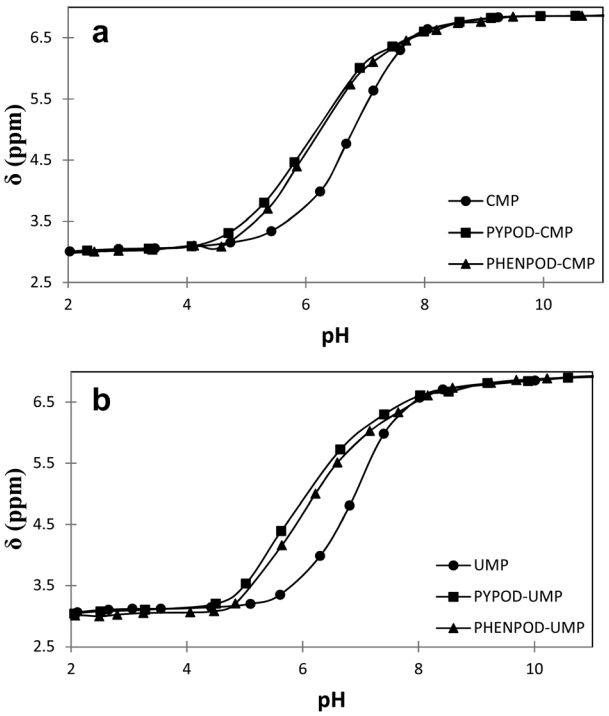

Fig. 4 Plot of ^{31}P NMR δ (ppm) *vs.* pH for free mononucleotides (●) CMP (a) and UMP (b) and for the complexes formed with PYPOD (■) and PHENPOD (▲).

(H_{R1}) of the nucleotide was also significantly shifted upfield upon complexation with **PYPOD**/**PHENPOD** (Fig. 5c).

An important fact is that the ^{1}H NMR shift differed in the acidic pH range, which varied considerably from pD ~ 1 only for **PHENPOD**–NMP systems, while no variation was observed for **PYPOD**–NMP systems until pD 2–3 depending on the system. This difference could be attributed to the stronger interactions exerted by **PHENPOD** based on a more effective aromatic stacking.

The ^{1}H NMR titrations of **PHENPOD** and **PYPOD** with the studied nucleotides at pD ~ 7.0 resulted in shifts of the proton signals, whereby the shift direction (upfield or downfield) as well as the intensity of the shifts varied significantly from case to case (examples Fig. 6, complete overview see ESI Table S4†). Although the large values of the stability constants prevented their determination by NMR titrations, and NOE experiments did not provide any relevant information, a qualitative analysis of the proton shifts can help to derive several general conclusions. For instance, the **PHENPOD**-AMP titrations (Fig. 6 UP) revealed strong shifts of the aromatic protons of both the ligand and the nucleobase, pointing toward pronounced aromatic stacking interactions – (a similar situation was observed also for other nucleotide complexes with **PHENPOD**), thus supporting the significant impact of the large phenanthroline ring in the binding. At variance to that, the **PYPOD**-nucleotide aromatic proton signal shifts (Fig. 6 DOWN) were smaller and more importantly, most of them shifted in the opposite direction than toward the **PHENPOD** systems, thus suggesting a

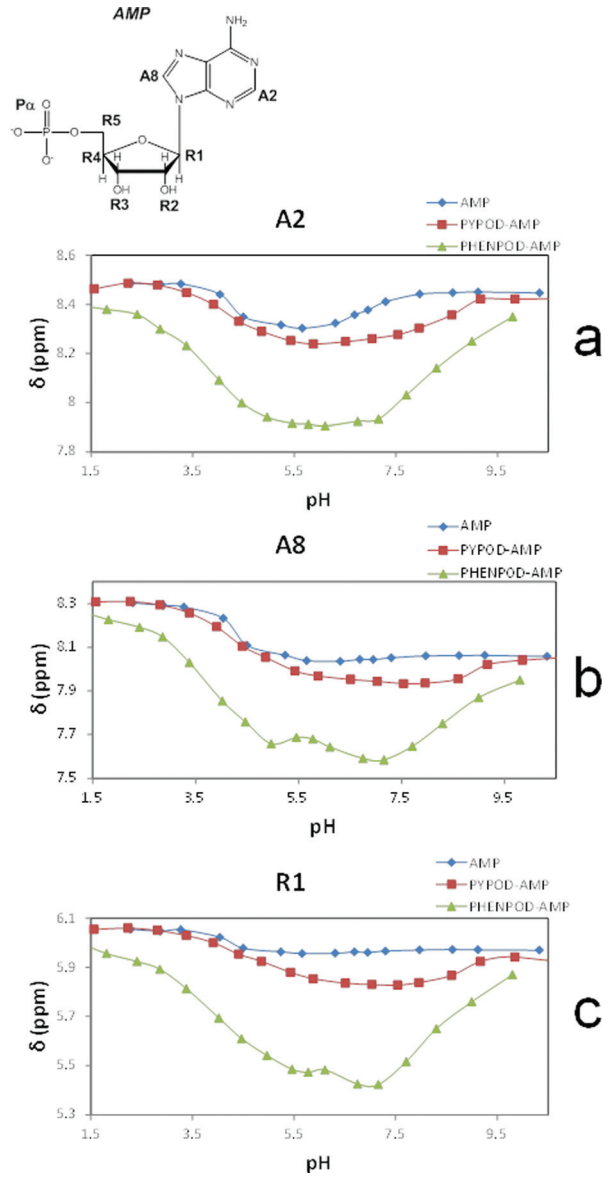

Fig. 5 Plot of ^{1}H NMR δ (ppm) *vs.* pH of: AMP complexes with **PYPOD** and **PHENPOD**: aromatic protons (a) H_{A2} and (b) H_{A8}, anomeric signal (c) H_{R1}.

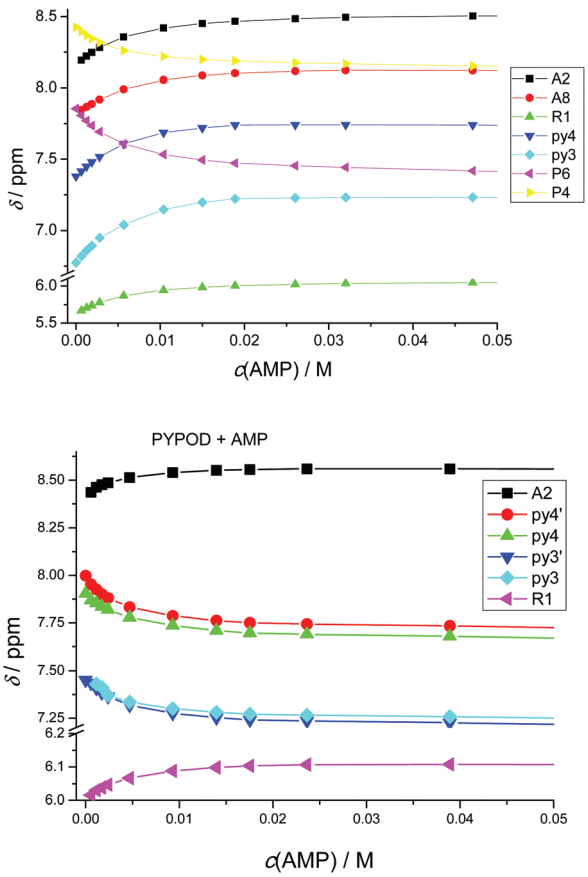

Fig. 6 ^{1}H NMR titration of **PHENPOD** (up) and **PYPOD** (down) with AMP, pD 6.8. For atom labelling see Scheme 1 and Fig. 5.

different combination of interactions and structural changes, whereby aromatic stacking (as expected) played only a minor role.

Molecular modelling. Since the NMR experiments did not provide direct information (intermolecular NOE cross-peaks) about the interactions between ligands and nucleotides, we combined all the aforementioned experimental data with molecular modelling in aqueous medium with the aim to relate the observed selectivity with the structure of the complexes formed. The phenanthroline derivative **PHENPOD** was omitted in the modelling studies because it showed similar affinity to all the studied nucleotide monophosphates with the exception of the selectivity towards AMP at acidic conditions, which was explained by protonation of the N1 of adenine[30] (a feature very challenging for computational studies because of the reversible positive charge at the heterocyclic moiety, which according to the NMR data was in stacking interaction with **PHENPOD**).

However, the **PYPOD**–NMP systems under neutral conditions were much more appropriate and interesting for modelling due to the selectivity found for CMP over UMP. Also, a close inspection of the hydrogen-bonding patterns revealed distinctive differences, which are summarized in Scheme 2. Such differences were particularly taken into account for the **PYPOD**–UMP system, which showed the lowest binding constant. Moreover, the small proton NMR shifts of the aromatic protons in the **PYPOD**–UMP system suggested that aromatic stacking interactions between the central pyridine of **PYPOD** and uracil could be neglected.

To start with, a **PYPOD** structure with four positive charges at the secondary ammonium nitrogens (according to the **PYPOD** protonation constants)[21] was constructed and minimised in aqueous medium (Fig. S13†). This **PYPOD** structure was used to construct the complexes with AMP, CMP and UMP. The molecular dynamics simulations revealed different features between the various complexes. The **PYPOD**–AMP complex appeared in several conformations and the two most abundant were characterised by aromatic stacking between

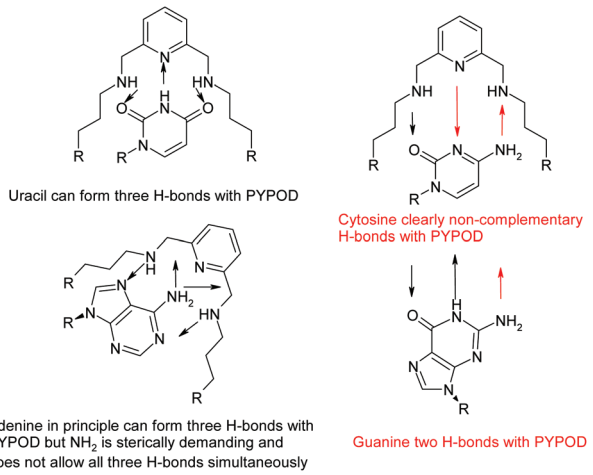

Scheme 2 Possibilities of H-bonding of nucleobases inside the **PYPOD**.

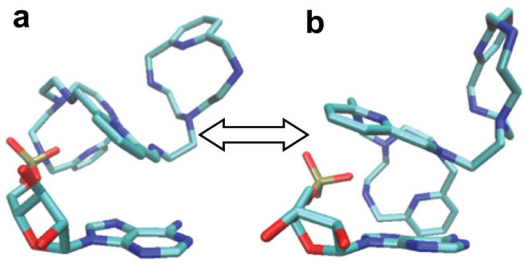

Fig. 7 Results of molecular dynamics simulations of the **PYPOD**–AMP complex: note the central pyridine–adenine orientation (a) approximately perpendicular; (b) approximately coplanar relation.

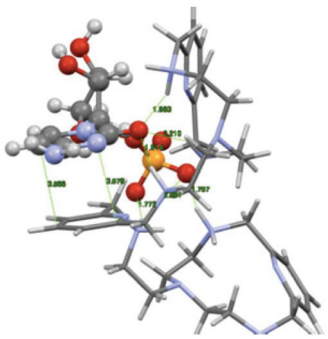

Fig. 8 Results of molecular dynamics simulations of **PYPOD**-CMP.

adenine and pyridine in either (a) approximately perpendicular or (b) approximately coplanar relation (Fig. 7a and 7b). Furthermore, the multiple electrostatic interactions between positively charged aliphatic nitrogens and negatively charged nucleotide phosphates (mostly located within the self-folded structure of the complex) additionally stabilised the system.

The **PYPOD**–CMP complex conformation obtained after 8 ns of distance constrained molecular dynamics simulation (for details see the Experimental section and ESI†) is shown in Fig. 8. The representative conformation was characterised by approximately coplanar stacking as well as more intensive electrostatic interactions in respect of the **PYPOD**–AMP complex. This is due to the more flexible self-folded structure of the complex caused by the smaller sized nucleobases, namely the larger adenine moiety which requires more space to accommodate in stacking with pyridine and consequently allows for less adjustment of the electrostatically interacting groups (phosphates *vs.* protonated amines). The minor impact of nucleobase aromatic stacking interactions on the overall stability of the complex is nicely demonstrated by similar binding constants of **PYPOD** with CMP and AMP despite the large difference in the nucleobase aromatic surface (cytosine has only half of the aromatic surface compared to, *e.g.*, adenine, and therefore usually exhibits an order of magnitude with a lower aromatic stacking affinity).

Intriguingly, the **PYPOD**–UMP complex unfolded during the molecular dynamics simulations, giving rise to a large number of quite different structures. Therefore, a novel starting complex structure was formed, taking into account a unique possibility of H-bond patterns (Scheme 2), and submitted to the molecular dynamics. As none of the obtained major conformations (Fig. S14, ESI†) showed significantly lower energy than the others, they could be discussed simultaneously. Essential for binding was the varying set of electrostatic interactions between the positively charged **PYPOD** side chains and the negatively charged UMP-phosphate; however H-bonding interactions of uracil also played an important role. Nevertheless, such multi-conformation sets resulted in relatively low overall stability in respect of the **PYPOD**–UMP complex.

Conclusions

The bis-polyazapyridinophane scorpiands **PYPOD** and **PHENPOD** efficiently bound the nucleotides in water by dominant electrostatic interactions between the nucleotide phosphates and the protonated aliphatic amines. Moreover, aromatic stacking interactions between the aryl groups of **PHENPOD**/**PYPOD** and the nucleobases also contribute to the binding. A similar synergistic effect of electrostatic and aromatic stacking interactions was recently reported for recognition in the AMP/ADP/ATP series.[12]

Intriguingly, fine regulation of the steric parameters in the scorpiand/nucleotide complex resulted in: (a) selectivity of **PYPOD** toward CMP in respect of other nucleotides (in particular UMP) based on the adjustment of the aromatic stacking partners with the electrostatic interaction partners as well as with the size and hydrophobicity of the **PYPOD** binding pocket; (b) selectivity of **PHENPOD** toward AMP under weakly acidic conditions based on the protonation of adenine heterocyclic N1. Both selectivities brought unparalleled features in the field of aqueous small molecule receptors for nucleotides.

Many small receptors recognised the purine (GMP and/or AMP) nucleotides by combined aromatic stacking interactions with electrostatic/H-bonding contribution within the receptor

pocket. Considering the pyrimidine nucleobases, mostly UMP/TMP selective receptors are reported, the selective interactions based on Zn^{2+}-coordination or complementary base recognition. The very recently reported unique example of TMP recognition (even in respect of the UMP) relied on a peculiar combination of binding interactions, including highly flexible aromatic macrocycle appended with a complementary base (adenine).[31] However, to the best of our knowledge, there is no low-molecular-weight receptor exhibiting preference toward CMP in respect of the other nucleotides. Therefore, particularly intriguingly, a two orders of magnitude higher affinity of **PYPOD** toward CMP in comparison with the other pyrimidine nucleotide (UMP) is observed here. There are several applications of such selectivity; for instance interfering with the action of sialyl transferases can be envisioned by the action of **PYPOD** selectively blocking the formation of CMP-sialic acid (enzyme donor substrate), in that way impairing the regulation of the sialylation of glycans on the cell surface.[32] Affinity of **PYPOD** toward AMP and GMP was slightly lower than toward CMP, pointing out the dominant impact of electrostatic interaction.

Furthermore, several AMP selective receptors are known,[33] but none of them has an on/off switchable mechanism so easily controlled as shown here for **PHENPOD**, which by pH change can ratiometrically switch on/off selectivity toward AMP in respect of other nucleotides (Fig. S9,† right: in mixture of all NMPs at pH 5 **PHENPOD** binds 72% of AMP, while at physiological pH 7.4 **PHENPOD** binds 40% of AMP).

Obtained selectivities are still not applicable for the efficient extraction of CMP or AMP from the mixture of nucleotides (including also di- and triphosphates, as well as other forms), however structure–activity relations are useful for further optimisation of **PHENPOD** and **PYPOD** as lead compounds. The design and study of new generations of analogues with delicately varied properties of aliphatic linkers (*e.g.* length, number and position of protonable amino groups) as well as variation of aryl-bridgesare in progress.

Experimental

All the reagents were supplied by commercial suppliers (Sigma-Aldrich) and analysed before using. The synthesis and characterization of **PYPOD** and **PHENPOD** have been described previously.[21]

EMF measurements

The potentiometric titrations were carried out at 298.1 ± 0.1 K using NaCl 0.15 M as a supporting electrolyte. The experimental procedure (burette, potentiometer, cell, stirrer, microcomputer, *etc.*) has been fully described elsewhere.[34] The acquisition of the EMF data was performed with the computer program PASAT.[35] The reference electrode was an Ag/AgCl electrode in saturated KCl solution. The glass electrode was calibrated as a hydrogen-ion concentration probe by titration of previously standardized amounts of HCl with CO_2-free NaOH solutions and the equivalent point determined by the Gran's method,[36] which gives the standard potential, $E°'$, and the ionic product of water ($pK_w = 13.73(1)$).

The computer program HYPERQUAD was used to calculate the protonation and stability constants.[26] The HYSS[37] program was used to obtain the distribution diagrams The pH range investigated was 2.5–11.0. In the binary L–A systems concentrations of the anion and of the receptors ranged from 1×10^{-3} M to 5×10^{-3} M.

NMR measurements

The ^1H and ^{13}C spectra were recorded on a Bruker AV 500 spectrometer at 500 MHz for ^1H and 125.43 MHz for ^{13}C. The NMR experiments involving ^{31}P were recorded on a Bruker AV 500 spectrometer equipped with a switchable probe. The chemical shifts were recorded in ppm. All spectra were recorded at room temperature and the concentration of **L1**·6HCl, **L2**·6HCl, AMP, GMP, UMP and CMP was 2×10^{-3} M in D_2O. The pD was adjusted using a concentrated solution of DCl or NaOD in D_2O.

Spectroscopic measurements

The emission fluorescence spectra were obtained on the Varian Eclipse fluorimeter in aqueous buffer solution (pH = 5, sodium cacodylate buffer, I = 0.05 M), all in quartz cuvettes (1 cm).

Molecular modelling

Initial structures of the ligand-mononucleotide complexes **PYPOD**-AMP, **PYPOD**-CMP and **PYPOD**-UMP were prepared using the program VMD1.8,[38] taking into account to the assumed electrostatic stabilizations shown in Scheme 2. The systems were parameterized by ANTECHAMBER and xLeaps, the modules available within the AMBER Tools, using the general AMBER force field GAFF.[39] The complexes were placed in the centre of the octahedral box filled with TIP3P type water molecules. A water buffer of 10 Å was used and Cl^- ions were added to neutralize the systems. The solvated complexes were geometry optimized in 2 cycles using the steepest descent and conjugate gradient methods with the solute molecules constrained by the harmonic potential. After optimization, systems were equilibrated for 2 ns in two steps: during the first step of 50 ps the system was heated from 0 to 300 K under NVT conditions. In the next step the water density was adjusted (NPT conditions). The equilibrated systems were subjected to the 4 ns of productive, unconstrained MD simulations at constant temperature (300 K) and pressure (1 atm) with the time step of 2 fs (SHAKE algorithm was used to restrain the motion of hydrogens). The simulations were performed with thesander program, available within the AMBER11 package,[40] using periodic boundary conditions, wherein the electrostatic interactions were calculated using the particle-mesh Ewald method.[41] The temperature and pressure was regulated using Langevin dynamics (with collision frequency of 1 ps-1) and the Berendsen barostat,[42] respectively. In the direct space the pairwise interactions were calculated

within the cut off distance of 11 Å. Since the complexes tended to fall apart (disintegrated), in further simulation of **PYPOD**–CMP and **PYPOD**–UMP complexes we used the weak distance constraints for the several **PYPOD**–UMP pairs of atoms (r_{up} = 3.55 Å, k_r = 10 kcal mol^{-1} Å^{-2}).

In total the complexes **PYPOD**–AMP, **PYPOD**–CMP and **PYPOD**–UMP were simulated for 14, 10 and 6 ns, respectively. The trajectories were visualized using the VMD 1.8 program.[38]

Acknowledgements

Financial support was received from Ministerio de Economia y Competitividad, FEDER and Generalitat Valenciana (Projects CTQ2009-14288-CO4-0, CONSOLIDER INGENIO 2010 CSD2010-00065 and PROMETEO 2011/008) and Ministry of Science, Education and Sport of Croatia (098-0982914-2918, 098-1191344-2860) are gratefully acknowledged. I. P. and E. G.-E. are grateful to COST Action CM1005 for their support in networking and mutual cooperation.

Notes and references

1 (*a*) E. Gendaszewska-Darmach and M. Kucharska, *Purigenic Signalling*, 2011, **7**, 193; (*b*) B. S. Khakh and G. Burnstock, *Sci. Am.*, 2009, **301**, 84; (*c*) W. G. Junger, *Nat. Rev. Immunol.*, 2011, **11**, 201.

2 M. Idzko, D. Ferrari and H. Eltschig, *Nature*, 2014, **509**, 310.

3 F. B. Chekeni, M. R. Elliott, J. K. Sandilos, S. F. Walk, J. M. Kinchen, E. R. Lazarowski, A. J. Armstrong, S. Penuela, D. W. Laird, G. S. Salvesen, B. E. Isakson, D. A. Bayliss and K. S. Ravichandran, *Nature*, 2010, **467**, 863.

4 E. R. Lazarowski, *Purigenic Signalling*, 2012, **8**, 359.

5 (*a*) J.-M. Lehn, *Supramolecular Chemistry. Concepts and Perspectives*, Wiley-VCH, Weinheim, 1995; (*b*) J. L. Atwood, *Comprehensive and Supramolecular Chemistry*, Pergamon, Oxford, 1996; (*c*) E. García-España, R. Belda, J. González, J. Pitarch and A. Bianchi, in *Receptor for Nucleotides. Supramolecular Chemistry: From Molecules to Nanomaterials*, ed. P. A. Gale and J. W. Steed, Wiley & Sons, 2012; (*d*) A. E. Hargrove, S. Nieto, T. Zhang, J. L. Sessler and E. V. Anslyn, *Chem. Rev.*, 2011, 6603.

6 (*a*) C. Bazzicalupi, A. Bencini, A. Bianchi, E. Faggi, C. Giorgi, S. Santarelli and B. Valtancoli, *J. Am. Chem. Soc.*, 2008, **130**, 2440; (*b*) C. Bazzicalupi, A. Bencini, S. Biagini, E. Faggi, S. Meini, C. Giorgi, A. Spepi and B. Valtancoli, *J. Org. Chem.*, 2009, **74**, 7349.

7 I. Tabushi, Y. Kobuke and J.-I. Imuta, *J. Am. Chem. Soc.*, 1981, **103**, 6152.

8 (*a*) B. Dietrich, M. W. Hosseini and J.-M. Lehn, *J. Am. Chem. Soc.*, 1981, **103**, 1282; (*b*) E. Kimura, M. Kodama and T. Yatsunami, *J. Am. Chem. Soc.*, 1982, **104**, 3182.

9 (*a*) A.-S. Delépine, R. Tripier, M. Le Baccon and H. Handel, *Eur. J. Org. Chem.*, 2010, 5380; (*b*) A.-S. Delepine, R. Tripier and H. Handel, *Org. Biomol. Chem.*, 2008, **6**, 1743.

10 (*a*) G. Malojčić, I. Piantanida, M. Marinić, M. Žinić, M. Marjanović, M. Kralj, K. Pavelić and H.-J. Schneider, *Org. Biomol. Chem.*, 2005, **3**, 4373; (*b*) A. Sornosa-Ten, M. T. Albelda, J. C. Frias, E. Garcia-Espana, J. M. Llinares, A. Budimir and I. Piantanida, *Org. Biomol. Chem.*, 2010, **8**, 2567.

11 (*a*) P. Arranz-Mascaros, C. Bazzicalupi, A. Bianchi, C. Giorgi, M. D. Gutierrez-Valero, R. Lopez-Garzon, M. L. Godino-Salido and B. Valtancoli, *Chem. Commun.*, 2011, **47**, 2814; (*b*) P. Arranz-Mascaros, C. Bazzicalupi, A. Bianchi, C. Giorgi, M. L. Godino-Salido, M. D. Gutierrez-Valero, R. Lopez-Garzon and B. Valtancoli, *New J. Chem.*, 2011, **35**, 1883.

12 H. Y. Kuchelmeister and C. Schmuck, *Chem. – Eur. J.*, 2011, **17**, 5311.

13 A. P. De Silva, H. Q. N. Gunaratne, T. Gunnlaugsson, A. J. M. Huxley, C. P. McCoy, J. T. Rademacher and T. E. Rice, *Chem. Rev.*, 1997, **97**, 1515.

14 (*a*) V. Kral and J. L. Sessler, *Tetrahedron*, 1995, **51**(2), 539; (*b*) J. L. Sessler, V. Kral, T. V. Shishkanova and P. A. Gale, *Proc. Natl. Acad. Sci. U. S. A.*, 2002, **99**, 4848.

15 Y. Hisamatsu, K. Hasada, F. Amano, Y. Tsubota, Y. Wasada-Tsutsui, N. Shirai, S. Ikeda and K. Odashima, *Chem. – Eur. J.*, 2006, **12**, 7733.

16 (*a*) L.-M. Tumir, M. Grabar, S. Tomić and I. Piantanida, *Tetrahedron*, 2010, **66**, 2501; (*b*) L.-M. Tumir, I. Piantanida, P. Novak and M. Žinić, *J. Phys. Org. Chem.*, 2002, **15**, 599; (*c*) I. Piantanida, B. S. Palm, P. Čudić, M. Žinić and H.-J. Schneider, *Tetrahedron Lett.*, 2001, **42**, 6779.

17 (*a*) M.-P. Teulade-Fichou, J.-P. Vigneron and J.-M. Lehn, *Supramol. Chem.*, 1995, **5**, 139; (*b*) O. Baudoin, F. Gonnet, M.-P. Teulade-Fichou, J.-P. Vigneron, J.-C. Tabet and J.-M. Lehn, *Chem. – Eur. J.*, 1999, **5**, 2762.

18 (*a*) M. Shionoya, T. Ikeda, E. Kimura and M. Shiro, *J. Am. Chem. Soc.*, 1994, **116**, 3848; (*b*) S. Aoki and E. Kimura, *J. Am. Chem. Soc.*, 2000, **122**, 4542.

19 (*a*) F. Schmidt, S. Stadlbauer and B. Konig, *Dalton Trans.*, 2010, **39**, 7250; (*b*) S. Aoki and E. Kimura, *J. Am. Chem. Soc.*, 2000, **122**, 4542.

20 M. Inclán, M. T. Albelda, E. Carbonell, S. Blasco, A. Bauz, A. Frontera and E. García-España, *Chem. – Eur. J.*, 2014, **20**, 3730.

21 J. González, J. M. Llinares, R. Belda, J. Pitarch, C. Soriano, R. Tejero, B. Verdejo and E. García-España, *Org. Biomol. Chem.*, 2010, **8**, 2367.

22 J. González-García, L. Uzelac, M. Kralj, J. M. Llinares, E. García-España and I. Piantanida, *Org. Biomol. Chem.*, 2013, **11**, 2154.

23 (*a*) J. A. Aguilar, E. García-España, J. A. Guerrero, S. V. Luis, J. M. Llinares, J. F. Miravet, J. A. Ramirez and C. Soriano, *J. Chem. Soc., Chem. Commun.*, 1995, 2237; (*b*) G. Kampf, L. E. Kapinos, R. Griesser, B. Lippert and H. Sigel, *J. Chem. Soc., Perkin Trans. 2*, 2002, 1320; (*c*) R. B. Martin and

Y. H. Mariam, *Met. Ions Biol. Syst.*, 1979, **8**, 57; (*d*) H. Sigel, *Pure Appl. Chem.*, 2004, **76**, 1869.

24 (*a*) H. A. Arab, Z. M. Anwar and M. Sokar, *J. Chem. Eng. Data*, 2004, **49**, 256; (*b*) Y. Kinjo, R. Tribolet, N. A. Corfù and H. Siegel, *Inorg. Chem.*, 1989, **28**, 1480.

25 (*a*) C. Frassineti, S. Ghelli, P. Gans, S. Sabatini, M. S. Moruzziy and A. Vacca, *Anal. Biochem.*, 1995, **231**, 374; (*b*) C. Frassineti, L. Alderighi, P. Gans, A. Sabatini, A. Vacca and S. Ghelli, *Anal. Bioanal. Chem.*, 2003, **376**, 1041; (*c*) L. Alderighi, A. Bianchi, L. Biondi, L. Calabi, M. D. Miranda, P. Gans, S. Ghelli, P. Losi, L. Paleari, A. Sabatini and A. Vacca, *J. Chem. Soc., Perkin Trans. 2*, 1999, 2741; (*d*) C. Frassineti, L. Alderighi, P. Gans, A. Sabatini, A. Vacca and S. Ghelli, *Anal. Bioanal. Chem.*, 2003, **376**, 1041.

26 P. Gans, A. Sabatini and A. Vacca, *Talanta*, 1996, **43**, 1739.

27 M. T. Albelda, J. Aguilar, S. Alves, R. Aucejo, P. Diaz, C. Lodeiro, J. C. Lima, E. García-España, F. Pina and C. Soriano, *Helv. Chim. Acta*, 2003, **86**, 3118.

28 (*a*) P. Job, *Comptes Rendus*, 1925, **180**, 928; (*b*) P. MacCarthy, *Anal. Chem.*, 1978, **50**, 2165.

29 (*a*) H. Y. Kuchelmeister and C. Schmuck, *Chem. – Eur. J.*, 2011, **17**, 5311; (*b*) O. Baudoin, F. Gonnet, M.-P. Teulade-Fichou, J.-P. Vigneron, J.-C. Tabet and J.-M. Lehn, *Chem. – Eur. J.*, 1999, **5**, 2762.

30 H. Sigel and R. Griesser, *Chem. Soc. Rev.*, 2005, **34**, 875.

31 M. Radić Stojković, M. Škugor, S. Tomić, M. Grabar, V. Smrečki, Ł. Dudek, J. Grolik, J. Eilmes and I. Piantanida, *Org. Biomol. Chem.*, 2013, **11**, 4077.

32 A. Maggioni, M. von Itzstein, I. B. R. Guzman, A. Ashikov, A. S. Stephens, T. Haselhorst and J. Tiralongo, *ChemBioChem*, 2013, **14**, 1936.

33 X.-F. Shang, H. Su, H. Lin and H.-K. Lin, *Inorg. Chem. Commun.*, 2010, **13**, 999.

34 E. García-España, M. J. Ballester, F. Lloret, J. M. Moratal, J. Faus and A. Bianchi, *J. Chem. Soc., Dalton Trans.*, 1988, 101.

35 M. Fontanelli and M. Micheloni, Proceedings of the I Spanish-Italian Congress on Thermodinamics of Metal Complexes, Peñíscola, Castellón, 1990. Program for the automatic control of the microburette and the acquisition of the electromotive force readings.

36 (*a*) G. Gran, *Analyst*, 1952, **77**, 661; (*b*) F. J. Rossotti and H. Rossotti, *J. Chem. Educ.*, 1965, **42**, 375.

37 P. Gans, *Programs to determine the distribution of Species in multiequilibria systems from the stability constants and mass balance equations*.

38 W. Humphrey, A. Dalke and K. Schulten, *J. Mol. Graphics*, 1996, **14**, 33.

39 W. D. Cornell, P. Cieplak, C. I. Bayly, I. R. Gould, K. M. Merz, D. M. Ferguson, D. C. Spellmeyer, T. Fox, J. W. Caldwell and P. A. Kollman, *J. Am. Chem. Soc.*, 1995, **117**, 5179.

40 D. A. Case, T. A. Darden, T. E. Cheatham III, C. L. Simmerling, J. Wang, R. E. Duke, R. C. Luo, W. Walker, W. Zhang, K. M. Merz, B. Roberts, B. Wang, S. Hayik, A. Roitberg, G. Seabra, I. Kolossváry, K. F. Wong, F. Paesani, J. Vanicek, J. Liu, X. Wu, S. R. Brozell, T. Steinbrecher, H. Gohlke, Q. Cai, X. Ye, J. Wang, M.-J. Hsieh, G. Cui, D. R. Roe, D. H. Mathews, M. G. Seetin, C. Sagui, V. Babin, T. Luchko, S. Gusarov, A. Kovalenko and P. A. Kollman, *AMBER 11*, University of California, San Francisco, 2010.

41 T. Darden, D. York and L. Pedersen, *J. Chem. Phys.*, 1992, **98**, 10089.

42 H. J. C. Berendsen, J. P. M. Postma, W. F. van Gunsteren, A. DiNola and J. R. Haak, *J. Chem. Phys.*, 1984, **81**(8), 3684.

